DOI: 10.1016/j.energy.2015.10.118

Exergetic Analysis of Hybrid Power Plants with Biomass and Photovoltaics Coupled with a Solid-Oxide Electrolysis System

Fontina Petrakopoulou[1,2,*], Javier Sanz-Bermejo[3], Javier Dufour[2,4], Manuel Romero[3]

[1]Department of Thermal and Fluid Engineering, Universidad Carlos III de Madrid, Avda. de la Universidad 30, 28911 Leganés (Madrid), Spain.

[2]Energy Systems Analysis Unit, Instituto IMDEA Energía, Avda. Ramón de la Sagra 3, 28933 Mostoles, Spain.

[3]Unit High-temperature Processes, Instituto IMDEA Energía, Avda. Ramón de la Sagra 3, 28933 Mostoles, Spain.

[4]Department of Chemical and Energy Technology, ESCET, Rey Juan Carlos University, Calle Tulipán s/n, 28933 Mostoles, Spain.

Abstract

This paper studies four hybrid systems that couple a reference –biomass and photovoltaic– power plant with four different structures of a steam electrolysis system for hydrogen production. The four hybrid plants are initially examined incorporating the same capacity components as the reference plant. The integration of different structures of the electrolysis process results in operational penalties when compared to the reference plant, due to added irreversibilities intrinsic to the electrolysis process and the reduction of the biomass plant efficiency from the extraction of low-pressure steam used to evaporate the electrolyzer feed water. The magnitude of these penalties depends on the power consumption of the electrolysis system, thermal demand and/or pressure losses within incorporated plant components. Among the alternative scenarios, the maximum efficiency is achieved when the electrolysis system uses a recycling sweep gas stream further used in the boiler of the biomass power plant. Furthermore, the efficiencies of the electrolysis hybrid plants only surpass that of the reference power plant when the solar

irradiation drops to 36-46 %. This is a direct result of the lower operational efficiency of the solar panels versus the biomass plant.

Keywords: intermediate temperature electrolysis, solid-oxide electrolysis cell (SOEC), biomass, photovoltaics, hybrid power plant, exergetic analysis

1 Introduction

The combination of biomass with photovoltaics (PV) can address problems that characterize the two technologies when they are used separately, such as daily and seasonal fluctuations of photovoltaic production and quality/quantity inconsistencies of biomass stock [1], [2]. Advantages of using biomass include, among others, its relatively lower environmental impact and its contribution towards independence from fossil fuels [3]. PV installations, on the other hand, operate without atmospheric emissions and are relatively easy to maintain [2]. Furthermore, hydrogen generation and storage options offer a possibility to further regulate the fluctuating output of renewable energy (e.g., [2]).

Water electrolysis is a power-driven process for generating hydrogen through the electrical decomposition of water into hydrogen and oxygen. It can be easily combined with infrastructure based on renewable energy sources. Hydrogen production systems using electricity generated in solar, wind, biomass and other energy conversion systems have been published in numerous studies (e.g., [4]–[10]). In addition, since 1991 several power-to-gas pilot plants have been constructed for producing hydrogen from renewable energy sources [11]. Most of these plants use alkaline or proton electrolyte membrane electrolyzers for hydrogen generation due to the maturity of this technology. However, the reported power consumption of water electrolysis is still above 4.5 kWh_{el}/Nm^3 of hydrogen [12].

The water split reaction can be described by the Gibbs function, $\Delta G = \Delta H - T \cdot \Delta S$, where ΔH is the overall energy needed, ΔG is the electrical energy and $T \cdot \Delta S$ is the direct heat.

Figure 1. Free energy water split diagram [13].

Solid-oxide electrolysis cell (SOEC) technology increases the operational temperature to above 600 °C in order to reduce the electrical requirements of the electrolysis process (see Figure 1).

High-temperature SOEC systems (HT-SOEC) in the range of 800–1000 °C have been studied since the 80s (e.g., [12], [14], [15]). Operation at high temperature reduces overpotentials and improves the activity of electrodes. As a result, the electricity demand can be reduced to 3.3 kWh_{el}/Nm^3 of hydrogen (at 1000 °C) and higher current densities can be achieved, improving the overall efficiency of hydrogen production and reducing the overall cost and size of the electrolyzer for a given production [12]. The cost can be further reduced if the heat requirement is covered by an external waste heat source [12], [16].

However, although high operating temperatures reduce the electrical requirement, they enhance chemical species evaporation and diffusion that reduce the performance and lifetime of the electrolyzer and decrease the mechanical stability of ceramic and metal components [17], [18]. HT-SOEC shortcomings are addressed by intermediate-temperature SOEC (IT-SOEC) [18]. IT-SOEC follow the trend of solid-oxide fuel cell (SOFC) technology that aims to reduce the operational temperature to 600-700 °C in order to decrease the equipment cost and increase the electrolyzer lifetime, while maintaining satisfactory performance levels [17], [18].

This work is based on the FP7 project ADEL that targeted the development of cost-competitive, energy efficient and sustainable hydrogen production based on renewable energy sources [13], [19].

2 Materials and Methods

This study evaluates the incorporation of different configurations of an IT-SOEC system into a reference PV-biomass power plant using exergetic analysis (e.g., [20], [21]). The electricity of the PV panels is used directly in the electrolyzer for the generation of hydrogen, while the electricity generated in the biomass plant can be used in the electrolyzer or delivered to the electrical grid, depending on the scenario examined. This work also evaluates the influence of PV capacity on the overall plant efficiency when keeping the capacities of the biomass plant and the electrolyzer constant. Thus, scenarios with acceptable PV-biomass ratios of electricity supply to the electrolyzer, i.e., with better performance than the reference plant, are revealed.

For the purpose of the presented work, the developed plants are planned to be located in an area with various chemical installations that rely on hydrogen availability. It is assumed that the hydrogen produced will be supplied to hydrotreatment processes of the refinery "La Rábida" constructed by the company CEPSA and located on the west side of the province of Huelva in Spain [22]. In addition, Huelva has significant biomass resources, produced both as a crop and as vegetable-matter wastes and by-products. The importance of biomass plants in the region is also proven by the fact that ENCE, Spain's leading company in biomass-fuelled renewable energy generation, already operates a large biomass power plant in the area with an electricity production of 68 MW_{el} [23].

The simulations are carried out at steady state conditions and they are performed using commercial software (EBSILONProfessional, [24]).

2.1 Reference PV-biomass power plant

The reference power plant represents a hybrid structure of a biomass plant with PV panels that generates 6.8 MW_{el}. The PV array generating 2.5 MW_{el} is based on the BP model 4180T and operates with an efficiency of 14.4 %. The biomass power plant is a conventional steam power plant with direct combustion of biomass generating 4.3 net MW_{el}. The configuration of the reference power plant can be seen in Figure 2.

The biomass plant uses 26.7 kton/year of hybrid poplar wood chips with a weight composition (dry) of 50.2 % C, 6.06 % H, 40.4 % O, 0.6 % N, 0.02 % S, 0.01 % Cl and 2.7 % ash [25]. The biomass (Stream 2 of Figure 2) is combusted with air in the boiler of the plant, providing thermal energy to convert water to superheated steam. The combustor of the biomass is assumed to be a second generation circulating fluidized bed boiler [26].

Steam generated at 80 bar and 550 °C (Stream 6) is expanded in the 3-pressure level steam turbine (ST) of the plant. One reheat stage is included before the intermediate-pressure steam turbine in order to increase the power output and the efficiency of the plant. At the last level of the steam turbine, the steam is expanded to 0.05 bar and it is led to the condenser (COND) of the plant (Stream 12). The saturated stream exiting the condenser (Stream 13) is passed through pumps and feedwater heaters entering the boiler at a temperature of 230 °C (Stream 5).

Figure 2. Theoretical reference PV-biomass power plant.

2.2 Electrolyzer Unit

The electrolyzer has been incorporated in all four hybrid scenarios examined; Its nominal power consumption is 500 kW_{el} and it consists of 110 parallel stacks, each one of which requires 4.5 kW. Defined and agreed upon among partners of the FP7 project ADEL [13],

it

is assumed that the electrolysis cells are working at thermoneutral voltage, at a temperature of 700 °C, with a steam conversion rate in the cathode chamber of 61 %, and a molar ratio between the anode and cathode of 1:1. Under these operational conditions, the overall energy efficiency of the electrolyzer, defined as the ratio between the lower heating value of the generated hydrogen and the stack power needed to perform this task, is 97.2 %.

2.3 Initial Layout of the Electrolysis System

In this study, a 2.5 MW_{el} electrolysis or IT-SOEC system composed of 5 500 kW-electrolyzers is simulated. The IT-SOEC system has been examined in four configurations (four scenarios). The operating conditions (Table 1), including pressure losses, efficiencies, minimum temperature differences, etc. of the electrolysis system are based on assumptions agreed upon by partners of the FP7 project ADEL [13].

TABLE 1. Operational characteristics of plant components.

Figure 3. Initial layout of the IT-SOEC system.

The initial layout of the IT-SOEC system consists of two loops (Figure 3). The first loop, which starts with Stream 46, provides the water entering the cathode side of the electrolysis process. In the second loop, atmospheric air (Stream 30) is used as sweep gas to remove the produced oxygen from the anode side of the electrolysis system.

In the first loop, the make-up water is pumped from 1.01 to 1.09 bar to overcome the pressure drops within the following processes. The water is heated up in shell-and-tube heat exchangers HX1 and HX2, the latter of which uses as thermal source steam extracted from the Rankine cycle of the biomass power plant. Mixer M2 mixes the make-up steam with Stream 42 (hydrogen-rich gas) to obtain a cathode inlet mixture of 10 % v/v

hydrogen and 90 % v/v steam (Steam 43). Heat exchanger HX3 (shell-and-tube) raises the temperature of the inlet steam/hydrogen mixture using as thermal source the exhaust cathode stream of the electrolysis system. Finally, the high-temperature electric heater EH1 is used to increase the temperature of the stream to the design operational temperature of the stacks (700 °C, Stream 45). EH1 is used to ensure adequate control of the inlet temperature of the stack given all operating conditions. In the electrolysis system, 61 % of the incoming H_2O is split into H_2 and O_2. The composition of the hydrogen/steam stream leaving the electrolysis process (Stream 37) is 65 % v/v hydrogen and 35 % v/v steam. This product stream is then routed through the recuperative heat exchangers, HX3 and HX1, to recover heat to improve the overall efficiency of the process. The hydrogen/steam exhaust stream is cooled down to 45 °C using the water-cooled heat exchanger HX4. The condensed water (Stream 54) is removed and the generated hydrogen, 1,050 ton/year of 90.5 % v/v H_2 and 9.5 % v/v H_2O (Stream 56), is stored.

The sweep-gas loop entering the anode is atmospheric air (Stream 30, molar composition 79.0 % N_2 and 21.0 % O_2). The blower COMP2 increases the pressure of the air sweep gas in order to overcome the pressure drops within the process. The air is filtered to remove suspended particles, and heated up by the exhaust anode stream (Stream 35) in HX5. A last electric heater EH2 is placed before the inlet of the IT-SOEC in order for the incoming stream to reach the required operational temperature.

Because the quality of the water used in the electrolyzer must be high, and since steam used in steam cycles may present traces of harmful compounds, the water of the electrolysis system is taken from an external source. In the simulations presented here, low-pressure steam extracted from the biomass power plant at 2.2 bar and 238 °C (Stream 28) is used indirectly to generate the steam required in the electrolyzer from a liquid clean water source. The condensed stream is finally returned to the biomass power plant

(Stream 29). Lastly, the electricity of the incorporated electric heat exchangers is supplied by the biomass power plant.

2.4 The hybridization scenarios

The first hybridization study considers the incorporation of the initial layout of the IT-SOEC system as described previously (Scenario 1, Figure 4). The second scenario examines the same structure of the IT-SOEC system with the difference that here exhaust air of the electrolysis unit (Stream 36 of Figure 5) is recirculated to the biomass combustor to further exploit its high temperature and oxygen content (Scenario 2, Figure 5). Scenario 3 examines the operation of the electrolysis system without sweep gas eliminating the need of an air compressor (Scenario 3, Figure 6). In Scenario 4 the electric heaters of the electrolysis system (EH1 and EH2) are replaced by gas/gas heat exchangers (HX6 and HX7) that use the exhaust gases of the combustion chamber as thermal input (Scenario 4, Figure 7).

In all of the simulations, the IT-SOEC system is provided with constant electricity supply (2.5 MW_{el}) and steam flow, assuring, in this way, constant hydrogen generation. The differences in electricity production among the scenarios stem mainly from differences in pressure losses and stream recirculation, which causes variations in temperature, combustion conditions and stream mixing. In the hybridization scenarios, the electricity required by the electrolysis system is covered fully by PV panels (2.5 MW_{el}), while the net electricity generated in the biomass plant (4.3 MW_{el}) is sent to the electrical grid.

Figure 4. Scenario 1: Hybrid plant incorporating the initial layout of the IT-SOEC system

Figure 5. Scenario 2: Variation of Scenario 1 (with air recirculation)

Figure 6. Scenario 3: Variation of Scenario 1 (elimination of the sweep gas of the electrolyzer unit)

Figure 7. Scenario 4: Variation of Scenario 2 (replacing the electric heat exchangers with gas/gas heat exchangers)

2.5 Sensitivity analysis of PV capacity

In order to examine the influence of variations of the PV output (due to transient conditions, e.g., passing clouds, sunrise and sunset) on the overall performance of the hybridization scenarios, different PV-biomass electricity supply ratios to the electrolysis system are investigated. This is achieved by assuming and testing various PV outputs from 0 to 100 % of the capacity of the electrolysis system (2.5 MW_{el}). In every case, the electricity generated in the PV panels is delivered to the electrolysis system exclusively. The biomass plant supplements the power input of the electrolysis system in order to reach the necessary 2.5 MW_{el}, and delivers the remaining power (up to 4.3 MW_{el}) to the electrical grid. For example, a 40/60 % PV-biomass ratio implies that 40 % of the electricity required in the electrolysis system is generated by the PV panels and the remaining 60 % by biomass combustion. This means that the capacity of the PV panels, and thus the electricity supplied to the electrolysis system using PV, is (0.4x2.5 MW_{el}) 1 MW_{el}. The biomass plant supplies the remaining required (2.5-1 MW_{el}) 1.5 MW_{el} and delivers the remaining power (4.3-1.5 MW_{el}) 2.8 MW_{el} to the electrical grid.

2.6 Exergetic analysis

The evaluation and comparison of the plants simulated and presented in this paper are realized using exergetic analysis. Energy can only be converted from one energy form to another, it is conserved and not destroyed. Exergy, on the other hand, is defined as the

maximum useful work during a process to bring a system into equilibrium with its environment [27]. The exergy of a stream depends on its state, and on the state of the environment; thus exergy destruction and exergy losses along a process can be quantified as functions of the quality of material streams. For this reason, exergy analysis is used to identify irreversibilities within components and systems, providing useful information for improving the thermodynamic performance of thermal processes [27].

The total exergy of a system results from the addition of physical exergy, kinetic exergy, potential exergy, and chemical exergy. In the present work kinetic and potential exergy terms are neglected. The chemical exergy of streams are calculated based on tabulated standard chemical exergies given by J. Szargut at standard conditions (T_0 = 298.15 K, P_0 = 1.013 bar) [28].

Defining the exergy of product, $E_{P,k}$, and the exergy of fuel, $E_{F,k}$, of a component k, we calculate its exergetic efficiency as $\varepsilon_k = E_{P,k} / E_{F,k}$. An exergy balance of a component quantifies the thermodynamic irreversibilities, i.e., the exergy destruction within the component: $E_{D,k} = E_{F,k} - E_{P,k}$.

The overall exergetic efficiency of the reference PV-biomass power plant is calculated as:

$$\varepsilon_{ref} = \frac{\left(\mathrm{P_{elec_{BP}}} + \mathrm{P_{elec_{PV}}}\right)}{\left(\mathrm{e_B} * \mathrm{m_B}\right) + \left[\frac{\mathrm{P_{elec_{PV}}}}{\varepsilon_{\mathrm{PV}}}\right]}$$

where BP: biomass plant, B: biomass, elec: electricity, e: specific exergy, m: mass flow, ε: exergetic efficiency, P: power and ref: reference.

In the case of the IT-SOEC hybrid plants, the exergy of the product (the numerator of the exergetic efficiency equation) of the reference plant will change for two reasons:(1)

hydrogen is generated in the introduced electrolyzer unit and (2) the electricity of the PV is used entirely as power input for the electrolyzer unit. When the PV output cannot fully cover the power requirement of the electrolyzer (due to low levels of irradiation), the additional power needed will be provided by the biomass plant (x_{BP}). Thus, the exergetic efficiency of the hybrid plants also incorporating the electrolysis system is defined as:

$$\varepsilon = \frac{\left(P_{elec_{BP}} - x_{BP} \cdot P_{elec_{IT-SOEC}}\right) + (e_{H2} * m_{H2})}{(e_B * m_B) + \left[\frac{P_{elec_{PV}}}{\varepsilon_{PV}}\right]}$$

where x_{BP}: the fraction of the electrical consumption of the electrolysis system supplied by the biomass plant.

3 Results and discussion

The results of the exergetic analysis at the component level for the reference power plant and the four hybridization scenarios can be seen in Tables 2-6. Results at the stream-level can be found in the Appendix of the paper. The exergy of the biomass stream has been calculated following the known procedure for solid fuels as mentioned in Ref. [27]. The solar exergy can be calculated using an energy/exergy ratio as presented in Ref. [29] that results in values very similar to its energy values. Here it was assumed that the exergy and energy values of solar energy are equal.

From the obtained results, it can be seen that the efficiencies of components with similar operation are comparable in all of the plants. Thus, any calculated changes in the overall efficiencies of the plants are associated with structural variations. It can be seen that the exergetic efficiency of some components is relatively low, when compared to similar components reported in literature [27]. For example, the air compressors operate with exergetic efficiencies of about 35 %, while the electric heaters in scenarios 1, 2 and 3

operate with exergetic efficiencies close to 66-67 %. The calculated irreversibilities of the components are closely related with the defined thermodynamic characteristics, i.e., isentropic efficiencies, pressure drops, temperature differences, etc., presented in Table 1. Thus, inefficiencies could be reduced through improved designs and the incorporation of components with better operational characteristics and lower thermodynamic inefficiencies.

TABLE 2. Component-level results of the exergetic analysis of the reference PV-biomass power plant.

TABLE 3. Component-level results of the exergetic analysis of Scenario 1 (with the initial layout of the IT-SOEC system.

TABLE 4. Component-level results of the exergetic analysis of Scenario 2 (sweep gas recycling).

TABLE 5. Component-level results of the exergetic analysis of Scenario 3 (no sweep gas).

TABLE 6. Component-level results of the exergetic analysis of Scenario 4 (replacement of the electric heat exchangers with gas/gas heat exchangers).

The efficiency of the reference PV-biomass plant is found to be 19.3 % based on dry biomass (Table 2). When comparing the hybridization scenarios with the reference PV-biomass power plant, it can be seen that the overall efficiency decreases by 6.3-7.5 %, depending on the structure of the IT-SOEC system. The reduction of the efficiency depends on two phenomena:

- With the integration of the IT-SOEC system, a small fraction of low-pressure steam is extracted from the steam turbine reducing the efficiency of the biomass power plant. In order to maintain the power output of the biomass power plant at the reference value (4.3 MW_{el}), the mass flow of the fuel has to be increased. This increases the exergy of the fuel of the system, which in turn is associated with a CO_2 increase of 15.9-16.0 ktons/year (assuming an annual operation of 7,446 hours).

- The electricity produced by the PV panels is now used in the integrated electrolysis process to generate hydrogen. The electrolysis process introduces new irreversibilities in the plants, reducing the exergy of the product of the overall system. Nevertheless, this is partially offset by the additional exergy gained from the generated hydrogen (Tables 3-6).

As mentioned, in Scenario 3 (Table 5) the sweep gas of the electrolysis system is eliminated in an attempt to decrease the power consumption of the overall structure. When comparing Scenario 1 (Table 3), that incorporates the initial layout of the IT-SOEC system, with Scenario 3, it can be seen that indeed the elimination of the sweep gas decreases the power consumption due to the elimination of the compressor covering the pressure losses within the filter, the heat exchangers and the electrolysis system, increasing the overall efficiency of the plant. Nevertheless, if, as in Scenario 2, the sweep gas is further recycled to the boiler of the biomass power plant (Table 4), the efficiency of the plant increases, surpassing that of Scenario 3. This is true because the benefit of the high-temperature oxygen-rich sweep gas in the biomass boiler is more significant than the decrease of the electricity consumption achieved in Scenario 3. In Scenario 4 (Table 6), the two electric heaters (EH1 and EH2) are replaced by gas/gas heat exchangers (HX6 and HX7) in an attempt to avoid the electricity consumption within the electrically driven heat exchangers. However, although the electricity required in the electric heaters is avoided and the efficiency of the plant is higher than for Scenario 1, the pressure losses of the flue-gas path are increased, increasing the requirements of the air compressor of the biomass

boiler. This eventually leads to an overall decrease in the energy efficiency of the plant, when compared with Scenario 2.

The results show that the overall efficiencies of the four examined scenarios are lower when PV panels are at full load, than during low irradiation periods (when part of the electricity needed in the electrolysis system is covered by the biomass plant). During low irradiation periods, the exergy of the product of the plant (electricity available to the grid) is reduced. However, these low irradiation levels strongly reduce the exergy of the fuel of the plant (thermal requirement), due to the low efficiency of the PV panels. The combination of these two effects causes an overall efficiency increase when irradiation levels decrease.

The performed sensitivity analysis shows that each scenario reaches the efficiency of the reference PV-biomass plant at different PV/biomass ratios. Specifically, it is found that Scenarios 3 and 4 result in efficiency higher than the reference PV-biomass power plant with a PV/biomass ratio of 39/61 %, i.e., maximum PV capacity of (0.39x2.5 MW_{el}) 0.975 MW_{el}. Scenario 1 requires a PV/biomass ratio of 36/64 %, i.e., maximum PV capacity of (0.36x2.5 MW_{el}) 0.9 MW_{el}. Lastly, Scenario 2 can supply up to 46 % of the electricity needs of the electrolysis system due to the relatively higher efficiency of the plant. This is translated to a maximum PV capacity of 1.15 MW_{el}. The above-mentioned results are shown in Figure 8.

Figure 8. Overall efficiency versus PV/biomass contribution ratio to the electricity needs of the electrolysis system.

4 Conclusions

From the realized simulations we found that coupling an intermediate temperature solid oxide electrolysis system (IT-SOEC) with a reference photovoltaic-biomass power plant

results in a reduction of the overall efficiency of 6.3-7.5 % relative to the reference case. This reduction is associated with (i) the transformation of electricity into hydrogen, which increases the irreversibilities throughout the process; and (ii) the reduction of the efficiency of the biomass plant due to the extraction of low-pressure steam used to evaporate the feed water of the electrolyzer. The efficiency reduction in the biomass plant is associated with an increase in CO_2 generation of 15.9-16.0 ktons/year (assuming annual operation of 7,446 hours) when the power output to the grid of the biomass plant is kept constant (4.3 MW_e).

Comparing four IT-SOEC integration schemes, we found that the incorporation of the intermediate-temperature electrolysis system with air recirculation (Scenario 2) performs with the highest efficiency. Although using a sweep gas is associated with additional power requirements, when recycled, the sweep gas has a positive effect on the combustion process of the biomass plant and, consequently, on the overall structure. This is mainly due to the high temperature of the recycled air and its high oxygen content. In addition, eliminating the electric heaters decreases the exergetic penalty of the processes. However, the pressure drop assumed within the gas/gas heat exchangers increases the power requirement of the compressors resulting in a lower efficiency than Scenario 2. If the pressure drop in these components was lower, the energy requirement of the main air compressor of this power plant structure would be reduced and its overall efficiency would increase. It should be mentioned that electric heaters have advantages over gas/gas heat exchangers, such as that they offer precise temperature control and low thermal inertia that results in fast transition processes, which can be useful when structures of high complexity are considered.

Lastly, when solar irradiation is below its reference value, the thermal input (exergy of fuel) decreases faster than the net power output of the biomass plant to the grid (exergy of product). This is due to the lower efficiency of the PV panels in comparison to the biomass

plant and results in an increase in the exergetic efficiency of the overall process. Specifically, it was found that when the solar irradiation is 36-46 %, the efficiency of the electrolysis hybrid plant is higher that of the reference PV-biomass power plant.

Acknowledgments

The authors would like to acknowledge the project ADEL co-funded by of the 7th Framework Programme of the European Union (FP7) and the Fuel Cells and Hydrogen Joint Undertaking (FCH-JU).

Fontina Petrakopoulou would like to thank the IEF Marie Curie Action PEOPLE-2012-IEF-GENERGIS-332028 funded by FP7.

Nomenclature

ε	Exergetic efficiency
$\dot{E}$	Exergy rate (MW)
p	Pressure (bar)
T	Temperature (°C)

Subscripts

CH	Chemical (exergy)
D	Exergy destruction
F	Fuel (exergy)
k	Component
P	Product (exergy)
PH	Physical (exergy)
tot	Overall system

Abbreviations

COMP	Compressor
COND	Condenser

1	EH	Electric heater
2	GEN	Generator
3	HX	Heat exchanger
4	IT-SOEC	Intermediate temprerature Solid oxide electrolyzer
5	M	Motor
6	P	Pump
7	PV	Photovoltaic
8	ST	Steam turbine
9	WPH	Water preheater

References

[1] Feedstock Ligistics Interagency Working Group, "Biofuel Feedstock Logistics: Recommendations for Research and Commercialization," 2011.

[2] R. Schleicher-Tappeser, "How renewables will change electricity markets in the next five years," *Energy Policy*, vol. 48, pp. 64–75, Sep. 2012.

[3] F. Delattin, J. De Ruyck, and S. Bram, "Detailed study of the impact of co-utilization of biomass in a natural gas combined cycle power plant through perturbation analysis," *Appl. Energy*, vol. 86, no. 5, pp. 622–629, May 2009.

[4] E. Erdle, J. Gross, and V. Meyringer, "Possibilities for hydrogen production by combination of a solar thermal central receiver system and high temperature electrolysis of steam," in *3rd Intl. workshop on solar thermal central receiver systems*, 1986, pp. 727–736.

[5] J. Sigurvinsson, C. Mansilla, P. Lovera, and F. Werkoff, "Can high temperature steam electrolysis function with geothermal heat?," *Int. J. Hydrogen Energy*, vol. 32, no. 9, pp. 1174–1182, Jun. 2007.

[6] R. Rivera-Tinoco, C. Mansilla, C. Bouallou, and F. Werkoff, "On the Possibilities of Producing Hydrogen by High Temperature Electrolysis of Water Steam Supplied from Biomass or Waste Incineration Units," *Int. J. Green Energy*, vol. 5, no. 5, pp. 388–404, 2008.

[7] H. Zhang, S. Su, X. Chen, G. Lin, and J. Chen, "Configuration design and performance optimum analysis of a solar-driven high temperature steam electrolysis system for hydrogen production," *Int. J. Hydrogen Energy*, vol. 38, no. 11, pp. 4298–4307, Apr. 2013.

[8] E. A. Harvego, M. G. McKellar, J. E. O'Brien, and J. S. Herring, "Parametric evaluation of large-scale high-temperature electrolysis hydrogen production using different advanced nuclear reactor heat sources," *Nucl. Eng. Des.*, vol. 239, no. 9, pp. 1571–1580, Sep. 2009.

[9] J. Sanz-Bermejo, J. Muñoz-Antón, J. Gonzalez-Aguilar, and M. Romero, "Optimal integration of a solid-oxide electrolyser cell into a direct steam generation solar tower plant for zero-emission hydrogen production," *Appl. Energy*, vol. 131, pp. 238–247, Oct. 2014.

[10] J. Sanz-Bermejo, J. Gallardo-Natividad, V. Gonzalez-Aguilar, and M. Romero, "Coupling of a Solid-Oxide cell unit and a linear Fresnel reflector field for grid management," *Energy Procedia*, vol. 57, pp. 706–715, 2013.

[11] G. Gahleitner, "Hydrogen from renewable electricity: An international review of power-to-gas pilot plants for stationary applications," *Int. J. Hydrogen Energy*, vol. 38, no. 5, pp. 2039–2061, Feb. 2013.

[12] T. Smolinka, *Encyclopedia of Electrochemical Power Sources*. Elsevier, 2009.

[13] "Project 'ADvanced ELectrolyser for Hydrogen Production with Renewable Energy Sources (ADEL).'" http://adel-energy.eu, 2012.

[14] W. Doenitz and R. Schmidberger, "Concepts and design for scaling up high temperature water vapour electrolysis," *Int. J. Hydrogen Energy*, vol. 7, no. 4, pp. 321–330, 1982.

[15] N. Mascalick, "High temperature electrolysis cell performance characterization," *Int. J. Hydrogen Energy*, vol. 11, no. 9, pp. 563–570, 1986.

[16] B. Yu, W. Zhang, J. Chen, J. Xu, and S. Wang, "Advance in highly efficient hydrogen production by high temperature steam electrolysis," *Sci. China Ser. B Chem.*, vol. 51, no. 4, pp. 289–304, Apr. 2008.

[17] M. S. Sohal, "Degradation in Solid Oxide Cells during High Temperature Electrolysis," 2009.

[18] A. Aguadero, L. Fawcett, S. Taub, R. Woolley, K.-T. Wu, N. Xu, J. A. Kilner, and S. J. Skinner, "Materials development for intermediate-temperature solid oxide electrochemical devices," *J. Mater. Sci.*, vol. 47, no. 9, pp. 3925–3948, Jan. 2012.

[19] O. Bucheli, F. Lefebvre-Joud, F. Petipas, M. Roeb, and M. Romero, "Advanced Electrolysers for Hydrogen Production with Renewable Energy Sources," in *Proceedings of the 10th European SOFC Forum*, 2012, p. A1107.

[20] F. Petrakopoulou, G. Tsatsaronis, T. Morosuk, and A. Carassai, "Conventional and advanced exergetic analyses applied to a combined cycle power plant," *Energy*, vol. 41, no. 1, pp. 146–152, Jul. 2012.

[21] F. Petrakopoulou, L. Y.D., and G. Tsatsaronis, "Simulation and Exergetic evaluation of CO_2 capture in a solid oxide fuel cell combined cycle power plant," *Appl. Energy*, vol. 114, pp. 417–425, 2013.

[22] "CEPSA-Refinery 'La Rábida,'" 2014. [Online]. Available: http://www.cepsa.com/cepsa/Who_we_are/The_Company/Activities/Refining/Refinery__La_Rabida_/. [Accessed: 15-Oct-2014].

[23] "ENCE," 2014. [Online]. Available: http://www.ence.es/en/energia-2/. [Accessed: 15-Oct-2014].

[24] SteagEnergyServices, "EBSILONProfessional," 2012. [Online]. Available: http://www.steag-systemtechnologies.com/ebsilon_professional.html. [Accessed: 21-Feb-2012].

[25] E. R. C. of the Netherlands, "Phyllis2 - ECN Phyllis classification," 2015. [Online]. Available: https://www.ecn.nl/phyllis2/Browse/Standard/ECN-Phyllis#butane. [Accessed: 27-May-2015].

[26] K. Niemelae and K. Westerlund, "Experience of fluidized bed technology for biomass plants in different applications and development towards new applications in RDF burning," in *PowerGen Europe*, 2003.

[27] A. Bejan, G. Tsatsaronis, and M. Moran, *Thermal Design and Optimization*. New York: Wiley-Interscience, 1996.

[28] J. Szargut, D. R. Morris, and F. R. Steward, *Exergy Analysis of Thermal, Chemical and Metallurgical Processes*. New York: Hemisphere Publishing Corporation, 1988.

[29] R. Petela, "Exergy of undiluted thermal radiation," *Sol. Energy*, vol. 74, no. 6, pp. 469–488, Jun. 2003.

Figure captions

Figure 1. Free energy water split diagram [13].

Figure 2. Theoretical reference PV-biomass power plant.

Figure 3. Initial layout of the IT-SOEC system.

Figure 4. Scenario 1: Hybrid plant incorporating the initial layout of the IT-SOEC system.

Figure 5. Scenario 2: Variation of Scenario 1 (with air recirculation).

Figure 6. Scenario 3: Variation of Scenario 1 (elimination of the sweep gas of the electrolyzer unit).

Figure 7. Scenario 4: Variation of Scenario 2 (replacing the electric heat exchangers with gas/gas heat exchangers).

Figure 8. Overall efficiency versus PV/biomass contribution ratio to the electrolyzer electricity needs.

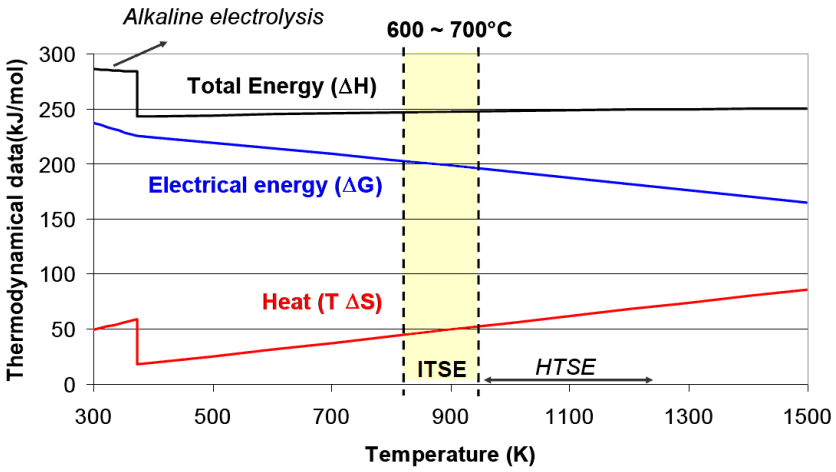
Alkaline electrolysis
600 ~ 700°C
Total Energy (ΔH)
Electrical energy (ΔG)
Heat (T ΔS)
ITSE
HTSE
Thermodynamical data(kJ/mol)
Temperature (K)
300
250
200
150
100
50
0
300
500
700
900
1100
1300
1500

1

2 **Figure 1**

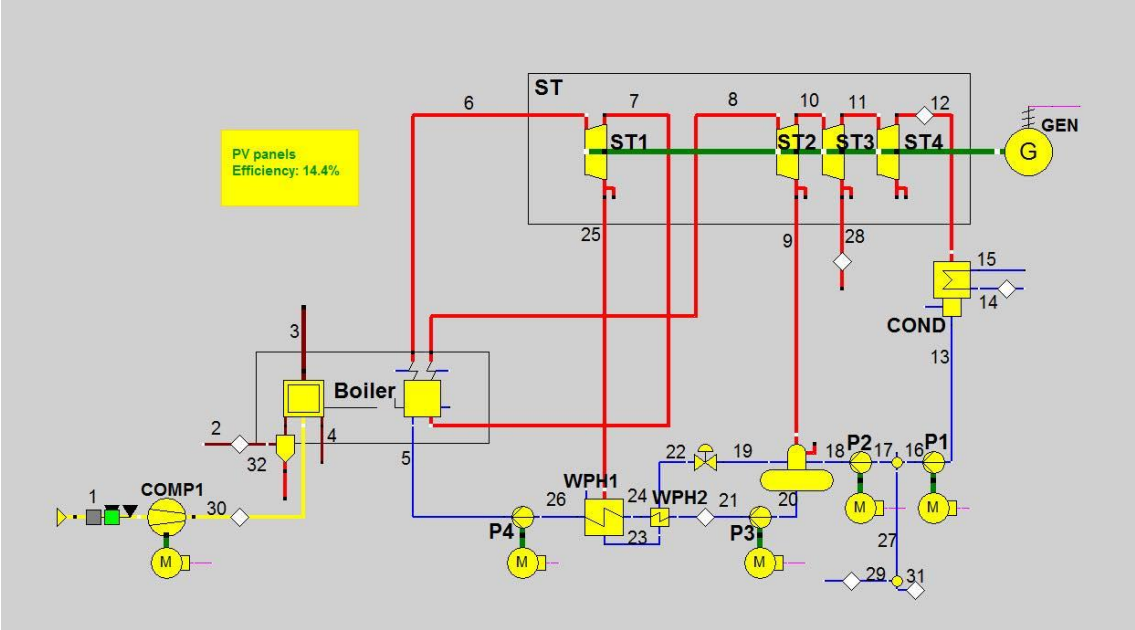
ST
ST1
ST2
ST3
ST4
GEN
G
PV panels
Efficiency: 14.4%
Boiler
COND
COMP1
WPH1
WPH2
P1
P2
P3
P4
M
1
2
3
4
5
6
7
8
9
10
11
12
13
14
15
16
17
18
19
20
21
22
23
24
25
26
27
28
29
30
31
32

Figure 2

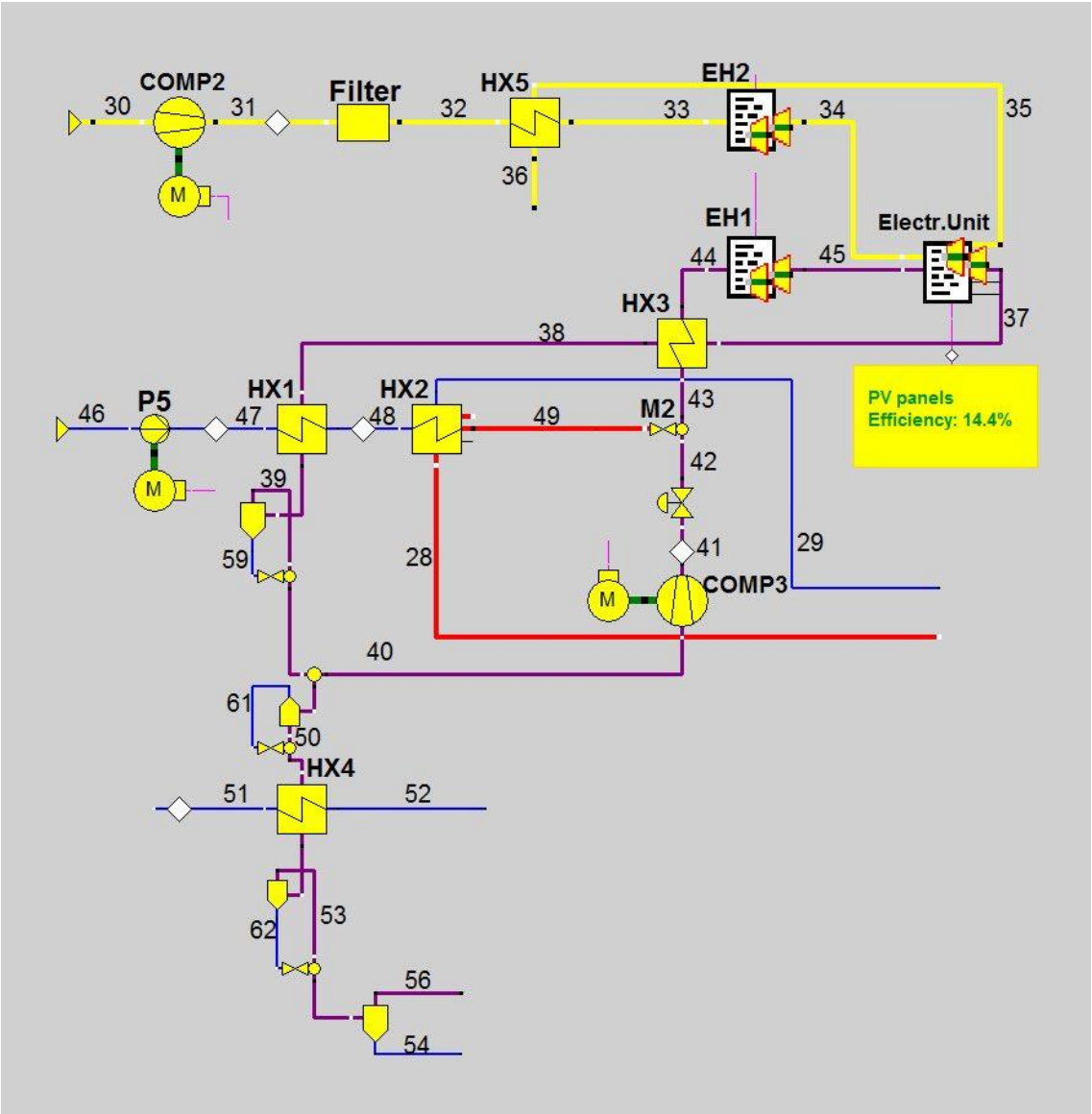
COMP2
Filter
HX5
EH2
EH1
Electr.Unit
HX3
HX1
HX2
P5
M2
COMP3
HX4
PV panels
Efficiency: 14.4%
30
31
32
33
34
35
36
37
38
39
40
41
42
43
44
45
46
47
48
49
50
51
52
53
54
56
59
61
62
28
29
M

Figure 3

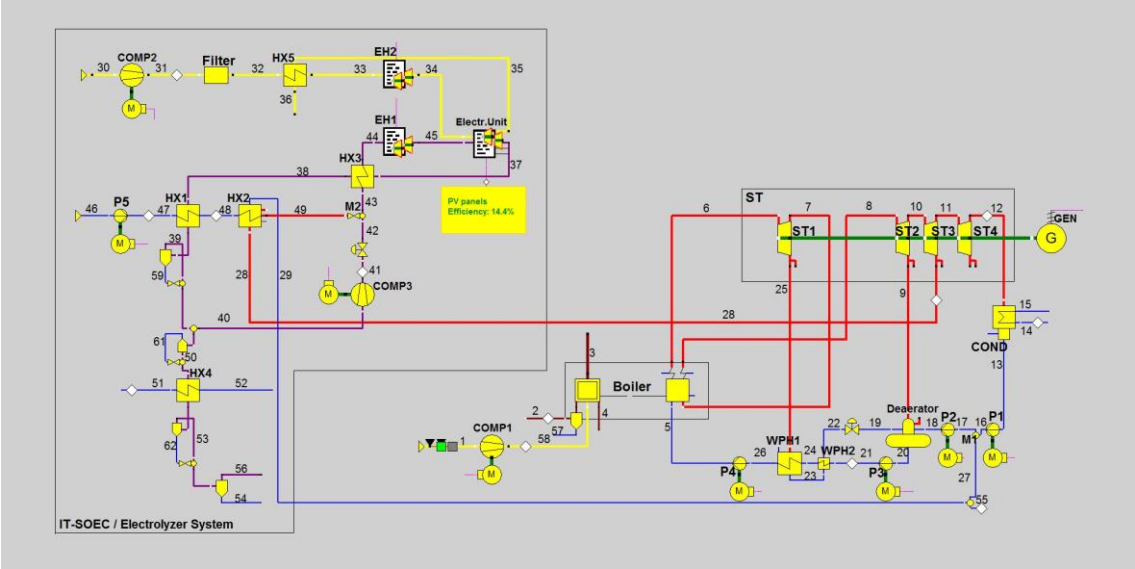
COMP2
Filter
HX5
EH2
EH1
Electr.Unit
HX3
PV panels
Efficiency: 14.4%
P5
HX1
HX2
M2
COMP3
HX4
ST
ST1
ST2
ST3
ST4
GEN
COND
Boiler
COMP1
Deaerator
P2
P1
M1
WPH1
WPH2
P4
P3
IT-SOEC / Electrolyzer System

Figure 4

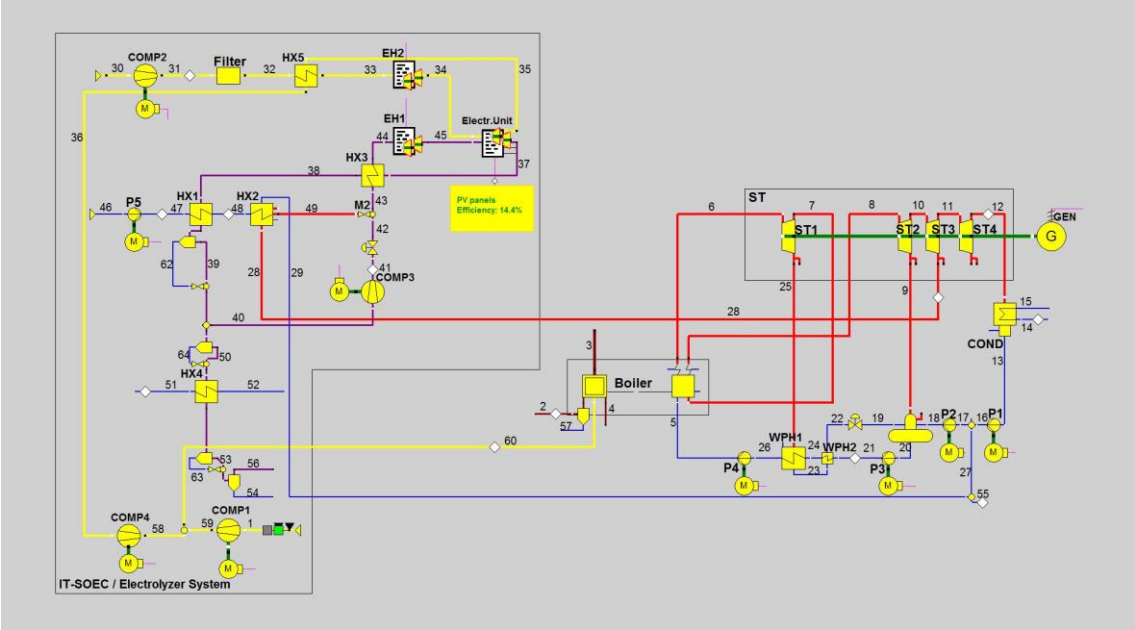
COMP2
Filter
HX5
EH2
EH1
Electr.Unit
HX3
HX1
HX2
P5
M2
COMP3
PV panels
Efficiency: 14.4%
ST
ST1
ST2
ST3
ST4
GEN
G
COND
Boiler
HX4
WPH1
WPH2
P1
P2
P3
P4
COMP4
COMP1
IT-SOEC / Electrolyzer System

Figure 5

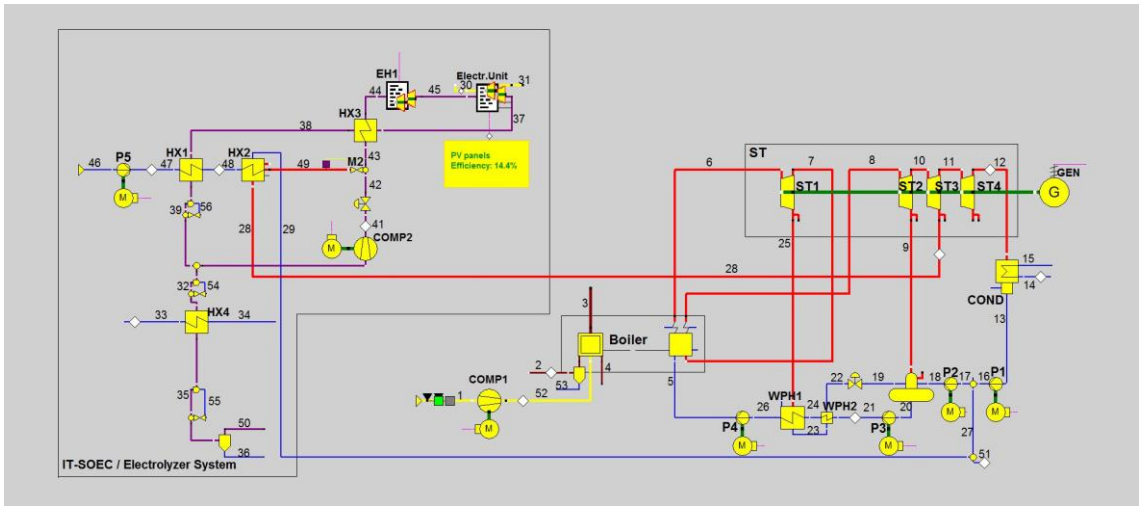
EH1
Electr.Unit
HX3
PV panels
Efficiency: 14.4%
P5
HX1
HX2
M2
COMP2
HX4
IT-SOEC / Electrolyzer System
ST
ST1
ST2
ST3
ST4
GEN
COND
Boiler
COMP1
WPH1
WPH2
P1
P2
P3
P4

Figure 6

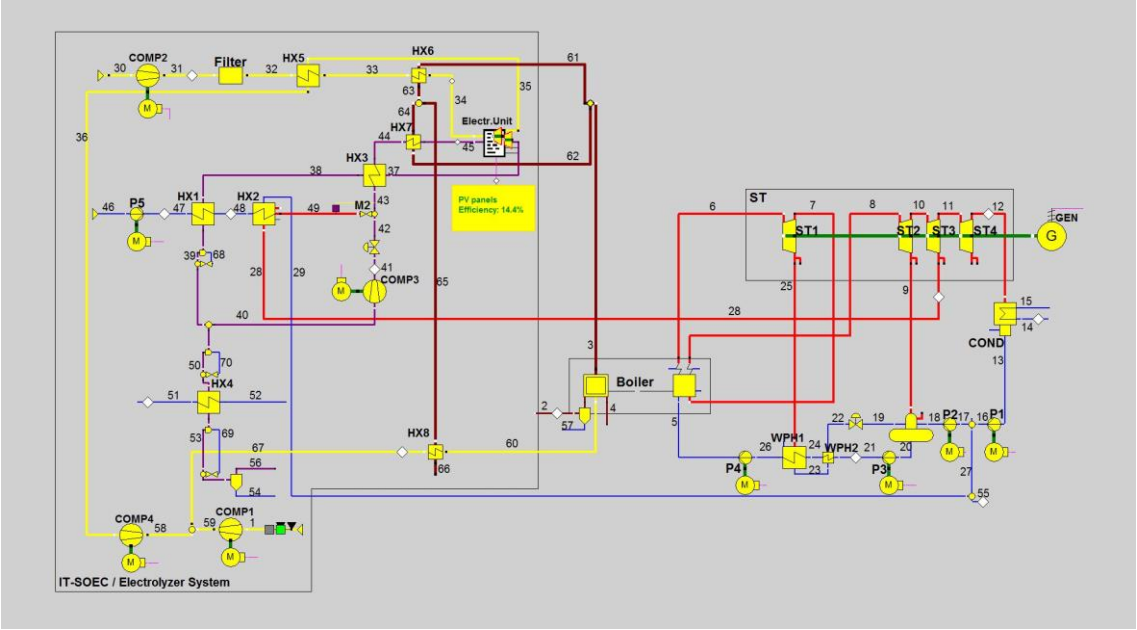
COMP2
Filter
HX5
HX6
Electr.Unit
HX7
HX3
PV panels
Efficiency: 14.4%
P5
HX1
HX2
M2
COMP3
HX4
HX8
Boiler
ST
ST1
ST2
ST3
ST4
GEN
G
COND
WPH1
WPH2
P4
P3
P2
P1
COMP4
COMP1
IT-SOEC / Electrolyzer System

Figure 7

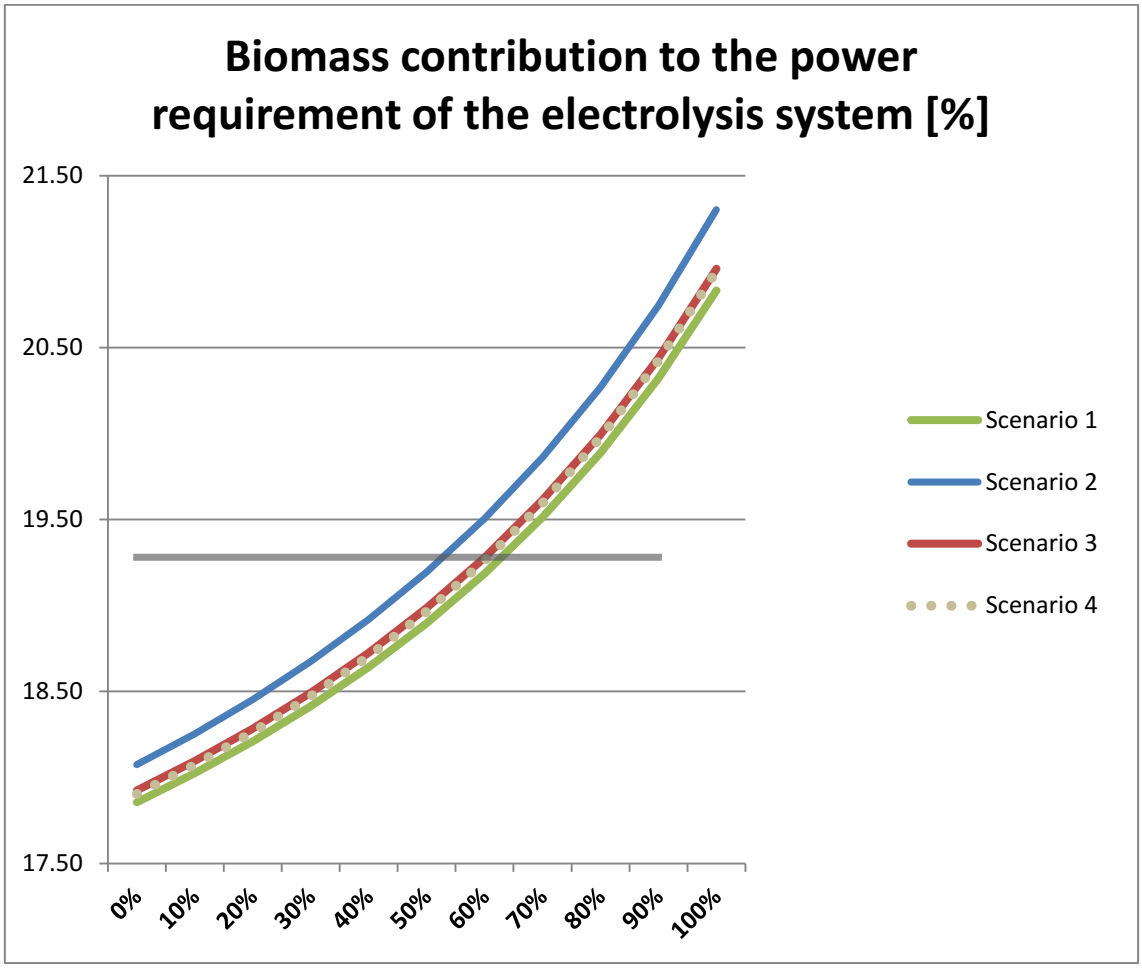
Biomass contribution to the power requirement of the electrolysis system [%]
21.50
20.50
19.50
18.50
17.50
0%
10%
20%
30%
40%
50%
60%
70%
80%
90%
100%
Scenario 1
Scenario 2
Scenario 3
Scenario 4

Figure 8

Table captions

TABLE 1. Operational characteristics of plant components.

TABLE 2. Component-level results of the exergetic analysis of the reference PV-biomass power plant.

TABLE 3. Component-level results of the exergetic analysis of Scenario 1 (with the initial layout of the IT-SOEC system.

TABLE 4. Component-level results of the exergetic analysis of Scenario 2 (sweep gas recycling).

TABLE 5. Component-level results of the exergetic analysis of Scenario 3 (no sweep gas).

TABLE 6. Component-level results of the exergetic analysis of Scenario 4 (replacement of the electric heat exchangers with gas/gas heat exchangers).

1 **TABLE 1**

BIOMASS & PHOTOVOLTAICS

Photovoltaic panels (PV)	
Model	BP 4180T
Electricity generation [kW]	2500.00
Electrical characteristics	
Maximum power at STC [W]	180.00
Voltage at Pmax (STC) [V]	35.80
Current at Pmax (STC) [A]	5.03
Module efficiency [%]	14.40
Nominal Voltage	24.00
Biomass power plant	
Combustion chamber	
Heat input by fuel [kW]	11986.84
Efficiency [%]	99.00
Pressure drop [bar]	0.15
Biomass LHV-AR [MJ/kg]	12.27
Boiler	
Outlet temperature, Stream 6 [°C]	550.00
Oulet pressure, Stream 6 [bar]	80.00
Steam turbine	
Inlet pressure, Stream 6 [bar]	80.00
Oulet pressure to condenser, Stream 12	0.05
Steam extractions, Streams 25/9/28	29.0/10.0/2.2
Isentropic efficiency [%]	88.0/88.0/88.0/91.0
Mechanical efficiency [%]	99.80
Efficiency of generator [%]	98.60
Condenser	
Working pressure [bar]	0.05
Pumps	
Isentropic efficiency [%]	75.00
Electrolyzer (Scenarios 1, 2, 3 and 4)	
Total capacity [kWel]	2503.00
Electricity demand [kWhe/Nm³ H2]	3.09
Steam conversion [%]	61.00
Operating temperature [°C]	700.00
H_2 at cathode inlet [%vol]	10.00
Sweep gas/cathode stream ratio	1:1
Pressure drop [mbar]	5.00

Other Equipment	
Electric heater (air, EH2)	
Pressure drop [mbar]	5.00
Electricity demand [kW]	12.10
Electric heater (H2-gas, EH1)	
Pressure drop [mbar]	5.00
Electricity demand [kW]	52.80
Air compressors	
Isentropic efficiency [%]	30.00
Mechanical efficiency [%]	95.00
H2 compressor	
Isentropic efficiency [%]	30.00
Mechanical efficiency [%]	95.00
Air preheater (HX5)	
Flow rate 32/35 [kg/s]	0.53/0.69
Temperature difference [°C]	20.00
Pressure drop cold side [mbar]	20.00
Pressure drop hot side [mbar]	30.00
Cathode gas preheater (HX3)	
Temperature difference [°C]	20.00
Pressure drop cold side [mbar]	20.00
Pressure drop hot side [mbar]	25.00
Water preheaters	
Gas preheater (HX1)	
Pressure drop cold side [mbar]	5.00
Pressure drop hot side [mbar]	5.00
Steam preheater (HX2)	
Temperature difference [°C]	20.00
Pressure drop cold side [mbar]	10.00
Pressure drop hot side [mbar]	10.00
H2 cooler (HX4)	
Pressure drop cold side [mbar]	5.00
Pressure drop hot side [mbar]	5.00

1 **Table 2**

Component				
COMP1	0.17	0.06	0.11	34.87
Boiler	9.43	5.56	3.86	59.03
PV panels	17.22	2.49	14.73	14.45
ST1	1.20	1.10	0.10	91.42
ST2	1.03	0.98	0.06	94.37
ST3	1.10	1.02	0.08	92.46
ST4	1.78	1.62	0.16	91.21
WPH1	0.33	0.30	0.04	89.40
WPH2	0.03	0.03	0.00	91.24
P1	0.00	0.00	0.00	73.51
P2	0.00	0.00	0.00	73.43
P3	0.02	0.02	0.00	81.12
P4	0.02	0.02	0.00	82.70
Deaerator	0.65	0.37	0.29	55.84
COND	0.17	-	0.17	-

Overall efficiency: 19.29 %

1 **Table 3**

Component				
COMP1	0.18	0.06	0.12	34.73
COMP2	0.01	0.00	0.01	31.70
COMP3	0.00	0.00	0.00	43.23
Boiler	9.69	5.72	3.97	59.03
Electr.Unit	2.49	2.29	0.19	92.18
PV panels	17.22	2.49	14.73	14.45
ST1	1.24	1.14	0.10	91.98
ST2	1.06	0.98	0.08	92.12
ST3	1.14	1.03	0.11	90.25
ST4	1.67	1.49	0.18	89.03
WPH1	0.34	0.30	0.04	89.40
WPH2	0.03	0.03	0.00	91.24
P1	0.00	0.00	0.00	73.85
P2	0.00	0.00	0.00	74.36
P3	0.02	0.02	0.00	81.61
P4	0.02	0.02	0.00	83.19
Deaerator	0.65	0.38	0.27	57.87
COND	0.16	-	0.16	-
HX5	0.21	0.18	0.03	83.43
EH1	0.05	0.04	0.02	66.81
EH2	0.01	0.01	0.00	66.32
HX1	0.02	0.01	0.02	35.94
HX2	0.18	0.15	0.03	83.81
HX3	0.17	0.16	0.01	94.49
HX4	0.00	0.00	0.00	0.00
M1	0.01	0.00	0.01	27.87
M2	0.39	0.38	0.01	97.31

Overall efficiency: 17.86 %

1 **Table 4**

Component				
COMP1	0.12	0.04	0.08	34.73
COMP2	0.01	0.00	0.01	31.70
COMP3	0.00	0.00	0.00	43.23
COMP4	0.05	0.03	0.02	59.09
Boiler	9.53	5.72	3.81	59.99
Eletr.Unit	2.49	2.29	0.19	92.18
PV panels	17.22	2.49	14.73	14.45
ST1	1.24	1.14	0.10	91.98
ST2	1.06	0.98	0.08	92.12
ST3	1.14	1.03	0.11	90.25
ST4	1.67	1.49	0.18	89.03
WPH1	0.34	0.30	0.04	89.40
WPH2	0.03	0.03	0.00	91.24
P1	0.00	0.00	0.00	73.85
P2	0.00	0.00	0.00	74.36
P3	0.02	0.02	0.00	81.61
P4	0.02	0.02	0.00	83.19
Deaerator	0.65	0.38	0.27	57.87
COND	0.16	-	0.16	-
EH2	0.01	0.01	0.00	66.32
EH1	0.05	0.04	0.02	66.81
HX1	0.02	0.01	0.02	35.94
HX2	0.18	0.15	0.03	83.81
HX3	0.17	0.16	0.01	94.49
HX4	0.02	0.00	0.02	0.00
HX5	0.21	0.18	0.03	83.43
M1	0.01	0.00	0.01	27.87

Overall efficiency: 18.07 %

1 **Table 5**

Component				
COMP1	0.18	0.06	0.12	34.73
COMP2	0.00	0.00	0.00	43.23
Boiler	9.69	5.72	3.97	59.03
Electr.Unit	2.49	2.31	0.17	92.98
PV panels	17.22	2.49	14.73	14.45
ST1	1.24	1.14	0.10	91.98
ST2	1.06	0.98	0.08	92.12
ST3	1.14	1.03	0.11	90.25
ST4	1.67	1.49	0.18	89.03
WPH1	0.34	0.30	0.04	89.40
WPH2	0.03	0.03	0.00	91.24
P1	0.00	0.00	0.00	73.85
P2	0.00	0.00	0.00	74.36
P3	0.02	0.02	0.00	81.61
P4	0.02	0.02	0.00	83.19
Deaerator	0.65	0.38	0.27	57.87
COND	0.16	-	0.16	-
EH1	0.05	0.04	0.02	66.81
HX1	0.02	0.01	0.02	35.94
HX2	0.18	0.15	0.03	83.81
HX3	0.28	0.16	0.13	55.26
HX4	0.02	0.00	0.02	0.00
M1	0.01	0.00	0.01	27.87
M2	0.39	0.38	0.01	97.31

Overall efficiency: 17.92 %

1 **Table 6**

Component				
COMP1	0.17	0.06	0.11	36.44
COMP2	0.01	0.00	0.01	31.70
COMP3	0.00	0.00	0.00	43.23
COMP4	0.06	0.04	0.03	60.10
Boiler	9.39	5.68	3.72	60.44
Electr.Unit	2.49	2.29	0.19	92.18
PV panels	17.22	2.49	14.73	14.45
ST1	1.23	1.13	0.10	91.98
ST2	1.05	0.97	0.08	92.12
ST3	1.13	1.02	0.11	90.25
ST4	1.66	1.48	0.18	89.03
WPH1	0.34	0.30	0.04	89.40
WPH2	0.03	0.03	0.00	91.24
P1	0.00	0.00	0.00	73.82
P2	0.00	0.00	0.00	74.36
P3	0.02	0.02	0.00	81.60
P4	0.02	0.02	0.00	83.19
Deaerator	0.64	0.37	0.27	57.88
COND	0.15	-	0.15	-
HX1	0.02	0.01	0.02	35.94
HX2	0.18	0.15	0.03	83.81
HX3	0.17	0.16	0.01	94.49
HX4	0.02	0.00	0.02	0.00
HX5	0.21	0.18	0.03	83.43
HX6	0.01	0.01	0.00	87.44
HX7	0.04	0.04	0.00	94.97
HX8	1.34	1.21	0.13	90.00
M1	0.01	0.00	0.01	27.91
M2	0.39	0.38	0.01	97.31
M3	0.01	0.01	0.00	99.63

Overall efficiency: 17.90 %

Appendix – Stream-level results of the exergetic analysis

TABLE A1. Stream-level results of the exergetic analysis of the reference PV-biomass power plant.

Stream, j		T	p			
	[kg/s]	[°C]	[bar]	[MW]	[MW]	[MW]
1	4.16	25.00	1.01	0.00	0.00	0.00
2	0.96	15.00	1.16	0.00	9.75	9.76
3	4.64	204.50	1.01	0.22	0.16	0.38
4	0.01	200.00	1.16	0.01	0.00	0.01
5	3.91	230.53	85.00	0.87	0.01	0.88
6	3.91	550.00	80.00	5.77	0.01	5.78
7	3.56	399.55	29.00	4.16	0.01	4.17
8	3.56	550.00	25.00	4.82	0.01	4.83
9	0.70	416.98	10.00	0.75	0.00	0.75
10	2.86	416.98	10.00	3.04	0.01	3.05
11	2.86	237.63	2.20	1.94	0.01	1.95
12	2.86	32.88	0.05	0.17	0.01	0.17
13	2.86	32.88	0.05	0.00	0.01	0.01
14	533.71	25.00	1.01	0.00	1.33	1.33
15	533.71	27.88	0.96	0.03	1.33	1.36
16	2.86	32.89	1.01	0.00	0.01	0.01
17	2.86	32.89	1.01	0.00	0.01	0.01
18	2.86	32.98	10.00	0.00	0.01	0.01
19	0.35	179.89	10.00	0.05	0.00	0.05
20	3.91	179.89	10.00	0.51	0.01	0.52
21	3.91	180.79	50.00	0.53	0.01	0.54
22	0.35	183.29	29.00	0.05	0.00	0.05
23	0.35	231.99	29.00	0.08	0.00	0.08
24	3.91	185.28	50.00	0.55	0.01	0.56
25	0.35	399.55	29.00	0.41	0.00	0.41
26	3.91	229.49	50.00	0.85	0.01	0.86
27	0.00	25.00	1.01	0.00	0.00	0.00
28	0.00	237.63	2.20	0.00	0.00	0.00
29	0.00	25.00	1.01	0.00	0.00	0.00
30	4.16	64.81	1.16	0.06	0.00	0.05
31	0.00	25.00	1.01	0.00	0.00	0.00
32	0.48	15.00	1.16	0.00	0.00	0.00

Biomass use (weight composition/dry: 50.2 % C, 6.06 % H, 40.4 % O, 0.6 % N, 0.02 % S, 0.01 % Cl and 2.7 % ash): 26,731 ton/year

TABLE A2. Stream-level results of the exergetic analysis of Scenario 1.

Stream. j		T	p			
	[kg/s]	[°C]	[bar]	[MW]	[MW]	[MW]
1	4,28	25,00	1,01	0,00	0,00	0,00
2	0,99	15,00	1,16	0,00	10,03	10,03
3	4,77	204,50	1,01	0,22	0,17	0,39
4	0,01	200,00	1,16	0,01	0,00	0,01
5	4,02	230,53	85,00	0,89	0,01	0,90
6	4,02	550,00	80,00	5,94	0,01	5,95
7	3,66	399,55	29,00	4,28	0,01	4,29
8	3,66	550,00	25,00	4,96	0,01	4,97
9	0,70	416,98	10,00	0,74	0,00	0,74
10	2,97	416,98	10,00	3,15	0,01	3,16
11	2,69	237,63	2,20	1,83	0,01	1,83
12	2,69	32,88	0,05	0,16	0,01	0,16
13	2,69	32,88	0,05	0,00	0,01	0,01
14	501,82	25,00	1,01	0,00	1,25	1,25
15	501,82	27,88	0,96	0,03	1,25	1,28
16	2,69	32,90	2,19	0,00	0,01	0,01
17	2,97	39,16	2,19	0,00	0,01	0,01
18	2,97	39,25	10,00	0,01	0,01	0,01
19	0,36	179,89	10,00	0,05	0,00	0,05
20	4,02	179,89	10,00	0,52	0,01	0,53
21	4,02	180,79	50,00	0,54	0,01	0,55
22	0,36	183,29	29,00	0,05	0,00	0,05
23	0,36	231,99	29,00	0,08	0,00	0,08
24	4,02	185,28	50,00	0,57	0,01	0,58
25	0,36	399,55	29,00	0,42	0,00	0,42
26	4,02	229,49	50,00	0,87	0,01	0,88
27	0,28	100,00	2,19	0,01	0,00	0,01
28	0,28	237,63	2,20	0,19	0,00	0,19
29	0,28	100,00	2,19	0,01	0,00	0,01
30	0,53	25,00	1,01	0,00	0,00	0,00
31	0,53	41,68	1,07	0,00	0,00	0,00
32	0,53	41,68	1,07	0,00	0,00	0,00
33	0,53	680,00	1,05	0,18	0,00	0,18
34	0,53	700,00	1,04	0,19	0,00	0,19
35	0,69	700,00	1,04	0,24	0,01	0,25
36	0,69	213,55	1,01	0,03	0,01	0,04
37	0,14	700,00	1,05	0,22	2,79	3,01
38	0,14	223,62	1,02	0,05	2,79	2,85
39	0,14	75,75	1,02	0,03	2,79	2,82
40	0,02	75,75	1,02	0,00	0,43	0,43
41	0,02	115,44	1,15	0,01	0,43	0,44
42	0,02	115,44	1,08	0,01	0,43	0,44
43	0,30	203,62	1,08	0,15	0,43	0,58
44	0,30	626,92	1,06	0,31	0,43	0,74
45	0,30	700,00	1,05	0,35	0,43	0,78
46	0,28	25,00	1,01	0,00	0,00	0,00
47	0,28	25,00	1,09	0,00	0,00	0,00
48	0,28	97,00	1,09	0,01	0,00	0,01
49	0,28	217,63	1,08	0,16	0,00	0,16
50	0,12	75,75	1,02	0,02	2,36	2,39
51	5,57	25,00	1,02	0,00	0,01	0,01
52	5,57	33,75	1,01	0,00	0,01	0,02
53	0,04	45,00	1,01	0,00	2,36	2,36
54	0,08	45,00	1,01	0,00	0,00	0,00
55	0,00	25,00	2,19	0,00	0,00	0,00

56	0,04	45,00	1,01	0,00	2,36	2,36
57	0,49	15,00	1,16	0,00	0,00	0,00
58	4,28	64,81	1,16	0,06	0,00	0,06
59	0,00	75,75	1,02	0,00	0,00	0,00
60	0,00	75,75	1,02	0,00	0,00	0,00
61	0,08	45,00	1,01	0,00	0,00	0,00
62	0,50	15,00	1,16	0,00	0,02	0,03
63	0,00	0,00	0,00	0,00	0,00	0,00

Biomass use (weight composition/dry: 50.2 % C, 6.06 % H, 40.4 % O, 0.6 % N, 0.02 % S, 0.01 % Cl and 2.7 % ash): 26,594 ton/year

H_2 production (9.5% H_2O, 90.5% H_2 v/v): 1,050 ton/year

TABLE A3. Stream-level results of the exergetic analysis of Scenario 2.

Stream, j		T	p			
	[kg/s]	[°C]	[bar]	[MW]	[MW]	[MW]
1	2,95	25,00	1,01	0,00	0,00	0,00
2	0,97	15,00	1,16	0,00	9,83	9,83
3	4,12	204,50	1,01	0,20	0,16	0,36
4	0,01	200,00	1,16	0,01	0,00	0,01
5	4,02	230,53	85,00	0,89	0,01	0,90
6	4,02	550,00	80,00	5,94	0,01	5,95
7	3,66	399,55	29,00	4,28	0,01	4,29
8	3,66	550,00	25,00	4,96	0,01	4,97
9	0,70	416,98	10,00	0,74	0,00	0,74
10	2,97	416,98	10,00	3,15	0,01	3,16
11	2,69	237,63	2,20	1,83	0,01	1,83
12	2,69	32,88	0,05	0,16	0,01	0,16
13	2,69	32,88	0,05	0,00	0,01	0,01
14	501,82	25,00	1,01	0,00	1,25	1,25
15	501,82	27,88	0,96	0,03	1,25	1,28
16	2,69	32,90	2,19	0,00	0,01	0,01
17	2,97	39,16	2,19	0,00	0,01	0,01
18	2,97	39,25	10,00	0,01	0,01	0,01
19	0,36	179,89	10,00	0,05	0,00	0,05
20	4,02	179,89	10,00	0,52	0,01	0,53
21	4,02	180,79	50,00	0,54	0,01	0,55
22	0,36	183,29	29,00	0,05	0,00	0,05
23	0,36	231,99	29,00	0,08	0,00	0,08
24	4,02	185,28	50,00	0,57	0,01	0,58
25	0,36	399,55	29,00	0,42	0,00	0,42
26	4,02	229,49	50,00	0,87	0,01	0,88
27	0,28	100,00	2,19	0,01	0,00	0,01
28	0,28	237,63	2,20	0,19	0,00	0,19
29	0,28	100,00	2,19	0,01	0,00	0,01
30	0,53	25,00	1,01	0,00	0,00	0,00
31	0,53	41,68	1,07	0,00	0,00	0,00
32	0,53	41,68	1,07	0,00	0,00	0,00
33	0,53	680,00	1,05	0,18	0,00	0,18
34	0,53	700,00	1,04	0,19	0,00	0,19
35	0,69	700,00	1,04	0,24	0,01	0,25
36	0,69	213,55	1,01	0,03	0,01	0,04
37	0,14	700,00	1,05	0,22	2,79	3,01
38	0,14	223,62	1,02	0,05	2,79	2,85
39	0,14	75,75	1,02	0,03	2,79	2,82
40	0,02	75,75	1,02	0,00	0,43	0,43
41	0,02	115,44	1,15	0,01	0,43	0,44
42	0,02	115,44	1,08	0,01	0,43	0,44
43	0,30	203,62	1,08	0,15	0,43	0,58
44	0,30	626,92	1,06	0,31	0,43	0,74
45	0,30	700,00	1,05	0,35	0,43	0,78
46	0,28	25,00	1,01	0,00	0,00	0,00
47	0,28	25,00	1,09	0,00	0,00	0,00
48	0,28	97,00	1,09	0,01	0,00	0,01
49	0,28	217,63	1,08	0,16	0,00	0,16
50	0,12	75,75	1,02	0,02	2,36	2,39
51	5,57	25,00	1,02	0,00	0,01	0,01
52	5,57	33,75	1,01	0,00	0,01	0,02
53	0,04	45,00	1,01	0,00	2,36	2,36
54	0,08	45,00	1,01	0,00	0,00	0,00
55	0,00	25,00	2,19	0,00	0,00	0,00

56	0,04	45,00	1,01	0,00	2,36	2,36
57	0,48	15,00	1,16	0,00	0,00	0,00
58	0,69	278,03	1,16	0,06	0,01	0,06
59	2,95	64,81	1,16	0,04	0,00	0,04
60	3,64	105,05	1,16	0,08	0,00	0,07
61	0,49	15,00	1,16	0,00	10,05	10,05
62	0,00	75,75	1,02	0,00	0,00	0,00
63	0,08	45,00	1,01	0,00	0,00	0,00

Biomass use (weight composition/dry: 50.2 % C, 6.06 % H, 40.4 % O, 0.6 % N, 0.02 % S, 0.01 % Cl and 2.7 % ash): 26,059 ton/year

H_2 production (9.5% H_2O, 90.5% H_2 v/v): 1,050 ton/year

TABLE A4. Stream-level results of the exergetic analysis of Scenario 3.

Stream, j		T	p			
	[kg/s]	[°C]	[bar]	[MW]	[MW]	[MW]
1	4,28	25,00	1,01	0,00	0,00	0,00
2	0,99	15,00	1,16	0,00	10,03	10,03
3	4,77	204,50	1,01	0,22	0,17	0,39
4	0,01	200,00	1,16	0,01	0,00	0,01
5	4,02	230,53	85,00	0,89	0,01	0,90
6	4,02	550,00	80,00	5,94	0,01	5,95
7	3,66	399,55	29,00	4,28	0,01	4,29
8	3,66	550,00	25,00	4,96	0,01	4,97
9	0,70	416,98	10,00	0,74	0,00	0,74
10	2,97	416,98	10,00	3,15	0,01	3,16
11	2,69	237,63	2,20	1,83	0,01	1,83
12	2,69	32,88	0,05	0,16	0,01	0,16
13	2,69	32,88	0,05	0,00	0,01	0,01
14	501,82	25,00	1,01	0,00	1,25	1,25
15	501,82	27,88	0,96	0,03	1,25	1,28
16	2,69	32,90	2,19	0,00	0,01	0,01
17	2,97	39,16	2,19	0,00	0,01	0,01
18	2,97	39,25	10,00	0,01	0,01	0,01
19	0,36	179,89	10,00	0,05	0,00	0,05
20	4,02	179,89	10,00	0,52	0,01	0,53
21	4,02	180,79	50,00	0,54	0,01	0,55
22	0,36	183,29	29,00	0,05	0,00	0,05
23	0,36	231,99	29,00	0,08	0,00	0,08
24	4,02	185,28	50,00	0,57	0,01	0,58
25	0,36	399,55	29,00	0,42	0,00	0,42
26	4,02	229,49	50,00	0,87	0,01	0,88
27	0,28	100,00	2,19	0,01	0,00	0,01
28	0,28	237,63	2,20	0,19	0,00	0,19
29	0,28	100,00	2,19	0,01	0,00	0,01
30	0,00	25,00	1,50	0,00	0,00	0,00
31	0,16	700,00	1,50	0,06	0,02	0,08
32	0,12	75,75	1,02	0,02	2,36	2,39
33	5,57	25,00	1,02	0,00	0,01	0,01
34	5,57	33,75	1,01	0,00	0,01	0,02
35	0,04	45,00	1,01	0,00	2,36	2,36
36	0,08	45,00	1,01	0,00	0,00	0,00
37	0,14	700,00	1,05	0,22	2,79	3,01
38	0,14	223,62	1,02	0,05	2,79	2,85
39	0,14	75,75	1,02	0,03	2,79	2,82
40	0,02	75,75	1,02	0,00	0,43	0,43
41	0,02	115,44	1,15	0,01	0,43	0,44
42	0,02	115,44	1,08	0,01	0,43	0,44
43	0,30	203,62	1,08	0,15	0,43	0,58
44	0,30	626,92	1,06	0,31	0,43	0,74
45	0,30	700,00	1,05	0,35	0,43	0,78
46	0,28	25,00	1,01	0,00	0,00	0,00
47	0,28	25,00	1,09	0,00	0,00	0,00
48	0,28	97,00	1,09	0,01	0,00	0,01
49	0,28	217,63	1,08	0,16	0,00	0,16
50	0,04	45,00	1,01	0,00	2,36	2,36

Biomass use (weight composition/dry: 50.2 % C, 6.06 % H, 40.4 % O, 0.6 % N, 0.02 % S, 0.01 % Cl and 2.7 % ash): 26,594 ton/year

H_2 production: (9.5% H_2O, 90.5% H_2 v/v): 1,050 ton/year

TABLE A5. Stream-level results of the exergetic analysis of Scenario 4.

Stream, j		T	p			
	[kg/s]	[°C]	[bar]	[MW]	[MW]	[MW]
1	3.00	25.00	1.01	0.00	0.00	0.00
2	0.98	15.00	1.22	0.00	9.94	9.94
3	4.18	720.00	1.07	1.69	0.17	1.85
4	0.01	200.00	1.22	0.01	0.00	0.01
5	3.99	230.53	85.00	0.89	0.01	0.90
6	3.99	550.00	80.00	5.89	0.01	5.90
7	3.64	399.55	29.00	4.25	0.01	4.26
8	3.64	550.00	25.00	4.92	0.01	4.93
9	0.69	416.98	10.00	0.73	0.00	0.74
10	2.95	416.98	10.00	3.13	0.01	3.14
11	2.67	237.63	2.20	1.81	0.01	1.82
12	2.67	32.88	0.05	0.15	0.01	0.16
13	2.67	32.88	0.05	0.00	0.01	0.01
14	497.75	25.00	1.01	0.00	1.24	1.24
15	497.75	27.88	0.96	0.03	1.24	1.27
16	2.67	32.90	2.19	0.00	0.01	0.01
17	2.95	39.21	2.19	0.00	0.01	0.01
18	2.95	39.29	10.00	0.01	0.01	0.01
19	0.36	179.89	10.00	0.05	0.00	0.05
20	3.99	179.89	10.00	0.52	0.01	0.53
21	3.99	180.79	50.00	0.54	0.01	0.55
22	0.36	183.29	29.00	0.05	0.00	0.05
23	0.36	231.99	29.00	0.08	0.00	0.08
24	3.99	185.28	50.00	0.57	0.01	0.58
25	0.36	399.55	29.00	0.42	0.00	0.42
26	3.99	229.49	50.00	0.87	0.01	0.88
27	0.28	100.00	2.19	0.01	0.00	0.01
28	0.28	237.63	2.20	0.19	0.00	0.19
29	0.28	100.00	2.19	0.01	0.00	0.01
30	0.53	25.00	1.01	0.00	0.00	0.00
31	0.53	41.68	1.07	0.00	0.00	0.00
32	0.53	41.68	1.07	0.00	0.00	0.00
33	0.53	680.00	1.05	0.18	0.00	0.18
34	0.53	700.00	1.04	0.19	0.00	0.19
35	0.69	700.00	1.04	0.24	0.01	0.25
36	0.69	213.55	1.01	0.03	0.01	0.04
37	0.14	700.00	1.05	0.22	2.79	3.01
38	0.14	223.62	1.02	0.05	2.79	2.85
39	0.14	75.75	1.02	0.03	2.79	2.82
40	0.02	75.75	1.02	0.00	0.43	0.43
41	0.02	115.44	1.15	0.01	0.43	0.44
42	0.02	115.44	1.08	0.01	0.43	0.44
43	0.30	203.62	1.08	0.15	0.43	0.58
44	0.30	626.92	1.06	0.31	0.43	0.74
45	0.30	700.00	1.05	0.35	0.43	0.78
46	0.28	25.00	1.01	0.00	0.00	0.00
47	0.28	25.00	1.09	0.00	0.00	0.00
48	0.28	97.00	1.09	0.01	0.00	0.01
49	0.28	217.63	1.08	0.16	0.00	0.16
50	0.12	75.75	1.02	0.02	2.36	2.39
51	5.57	25.00	1.02	0.00	0.01	0.01
52	5.57	33.75	1.01	0.00	0.01	0.02
53	0.04	45.00	1.01	0.00	2.36	2.36
54	0.08	45.00	1.01	0.00	0.00	0.00
55	0.00	25.00	2.19	0.00	0.00	0.00

56	0.04	45.00	1.01	0.00	2.36	2.36
57	0.49	15.00	1.22	0.00	0.00	0.00
58	0.69	300.11	1.22	0.07	0.01	0.07
59	3.00	78.94	1.22	0.06	0.00	0.06
60	3.69	687.58	1.22	1.31	0.00	1.31
61	2.09	720.00	1.07	0.84	0.08	0.93
62	2.09	720.00	1.07	0.84	0.08	0.93
63	2.09	715.37	1.06	0.83	0.08	0.92
64	2.09	699.79	1.06	0.81	0.08	0.89
65	4.18	707.58	1.06	1.64	0.17	1.81
66	4.18	249.32	1.06	0.30	0.17	0.46
67	3.69	120.22	1.22	0.11	0.00	0.10
68	0.00	75.75	1.02	0.00	0.00	0.00
69	0.08	45.00	1.01	0.00	0.00	0.00
70	0.00	75.75	1.02	0.00	0.00	0.00

Biomass use (weight composition/dry: 50.2 % C, 6.06 % H, 40.4 % O, 0.6 % N, 0.02 % S, 0.01 % Cl and 2.7 % ash): 26,356 ton/year

H_2 production: (9.5% H_2O, 90.5% H_2 v/v): 1,050 ton/year